

Effect of Body Motion and the Type of Antenna on the Measured UWB Channel Characteristics in Medical Applications of Wireless Body Area Networks

Attaphongse Taparugssanagorn, *Member, IEEE*, Carlos Pomalaza-Ráez, *Senior Member, IEEE*, Raffaello Tesi, *Member, IEEE*, Matti Hämäläinen, *Member, IEEE*, and Jari Iinatti, *Senior Member, IEEE*

Centre for Wireless Communications, University of Oulu, Finland

Abstract—Wireless body area networks (WBAN) are being considered as one of the most suitable technologies for remote health monitoring. This technology has the potential to increase the quality of medical care as well as keeping under control the associated costs. Due to the complex shape of the human body and its different tissues it is expected that the propagation characteristics of the radio channel, when measured in close proximity of a human body, to be different than those found in other scenarios. The work described in this papers aims to expand the knowledge of the ultra-wideband (UWB) channel in the frequency range of 3.1-10 GHz, for the case of WBANs, under static and dynamic scenarios. Two different type of antennas are used, the SkyCross SMT-3TO10M-A and the P200 BroadSpec™. To minimize the effects of the environment the measurements were conducted in an anechoic chamber.

I. INTRODUCTION

Advances in wireless technology have led to the development of wireless body area networks (WBAN) [1] where a set of communication devices are deployed in close proximity and around a human body. In medical applications these devices are connected to sensors that can monitor vital signs such as ECG and temperature as well as motion, greatly facilitating what is generally known as wireless medical telemetry [2]. Using a WBAN it is possible to remotely monitor a patient's health status minimizing the number of cables and devices needed. The use of this technology has the potential to reduce the costs of health care by decreasing the need to have medical and technical staff physically close to patients at all times. Among the several competing wireless technologies Ultra-wideband (UWB) communications is a very promising one for WBAN due to its particular characteristics [3, 4]. The monitoring of human vital signs and motions requires a relatively low data rate which in the case of UWB translates into very small transmitting power requirements, i.e., longer battery life and less potential side effects caused by the electromagnetic radiation. These are very desirable features for devices that are going to be close to the body and meant to be used for extended periods of time. To properly design and develop UWB devices for use in WBANs it is necessary to know the characteristics of the radio propagation channel

in close proximity to a human body. For the case of generic indoor and outdoor scenarios comprehensive studies of the UWB propagation channel have been already performed in recent years [3, 5, 6]. It is natural to expect that the channel characteristics for those cases will be different than the ones found in WBAN scenarios due to the effect of the human body with its complex shape and different tissues, each with a different permittivity [7]. UWB measurements around the human body have been carried out by various researchers [8-10]. Those experiments have been limited to scenarios that are not likely to take place in medical applications, e.g. numerous antennas located around the whole body, antennas in close contact to skin, etc. The main contribution of the work reported in this paper are: (a) experimental measurements of the UWB channel, in an anechoic chamber, with a static and dynamic body in situations more likely to take place in a medical application, and (b) study of the effect of using different types of antennas, namely, the SkyCross SMT-3TO10M-A and the P200 BroadSpec™ antennas. The scenarios under consideration include the radio links between sensor nodes themselves and between a sensor node to a control node or gateway few meters from the body [3], e.g., on a wall or the ceiling as shown in Fig. 1.

II. CHANNEL MEASUREMENT SETUP AND SCENARIOS

The channel measurement system described in this paper consists of an HP Agilent 8720ES [11], a vector network analyzer (VNA), SkyCross SMT-3TO10M-A antennas [12] and P200 BroadSpec™ antennas [13], 5-m long SUCOFLEX® RF cables [14] with 7.96 dB loss and a control computer with LabVIEW™ 7 software. As shown in Fig. 2, the P200 BroadSpec™ antenna is twice larger than the SkyCross SMT-3TO10M-A antenna. The SkyCross SMT-3TO10M-A antennas and the P200 BroadSpec™ antennas are azimuthally omnidirectional with their radiation patterns as shown in [12-13]. Both SkyCross and BroadSpec™ antennas are quite well matched with Voltage Standing Wave Ratio (VSWR) < 2 : 1 across 3.6-9.1 GHz and $\sim 1.5 : 1$ through across 3.0-5.5 GHz, respectively and radiation efficient. Both antennas offers

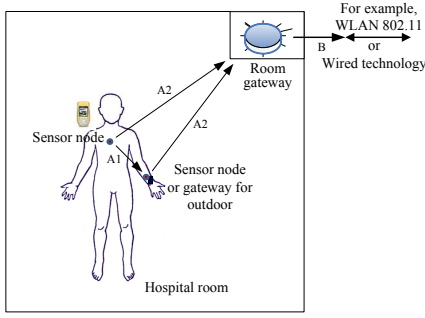


Fig. 1. (A) The WBAN channels: (A1) the channels between sensor nodes themselves and (A2) the channel from a sensor node to a gateway. (B) the channel from a gateway to some other wireless networks.

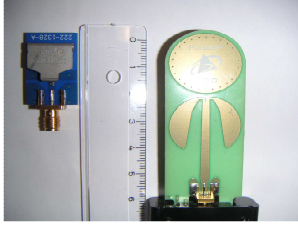


Fig. 2. SkyCross, SMT-3TO10M-A antenna (left) and BroadSpec™ antennas (right).

a very linear phase response. The VNA is operated in a transfer function measurement mode, where port 1 and port 2 are the transmitting and the receiving ports, respectively. This corresponds to a S_{21} -parameter measurement set-up, where the device under test (DUT) is the radio channel. The frequency band used in the measurements is from 3.1-10 GHz, which is the entire frequency range of the antennas. Therefore, the bandwidth B is 6.9 GHz. The maximum number of frequency points per sweep M is 1601, which can then be used to calculate the maximum detectable delay τ_{\max} of the channel as

$$\tau_{\max} = (M - 1)/B. \quad (1)$$

Using (1), the maximum detectable delay, τ_{\max} of the channel is 231 ns, which corresponds to 69.3 m in free space distance. Here we are interested in the first 20 ns, i.e., at most 6 m away from the body. We have learned in [15-16] that the radio link is significantly improved with a dielectric separation between the body and the antennas. This is also a more realistic situation in a medical application, i.e., there is no reason why the antenna has to be very close to the skin. Therefore, a 1.2 cm dielectric separation is used for all the experiments described in this paper. The measurements setups are designed with more realistic scenarios in mind. This means that the number of antennas near the body is small. Also, only comfortable locations on the body where to place the antennas are selected. The transmit (Tx) power is 1 mW (0 dBm), the same as the Bluetooth class 3 radiation power.

The UWB channel measurement experiments were conducted in an anechoic chamber to minimize other effects

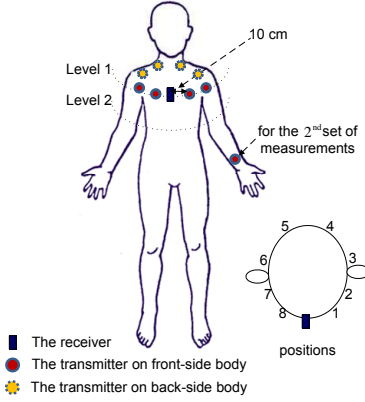


Fig. 3. Antenna positions for the 1st and the 2nd sets of measurements.



Fig. 4. Each position of a walking cycle.

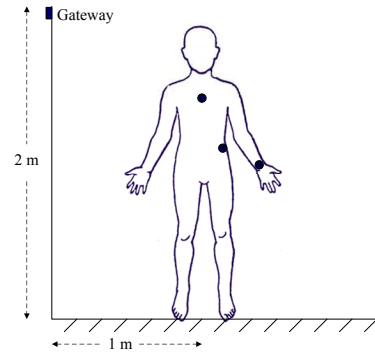


Fig. 5. Antenna position for the 3rd set of measurements when the subject is facing the Rx antenna. The rectangle and the circle represent the Rx antenna and the Tx antenna, respectively.

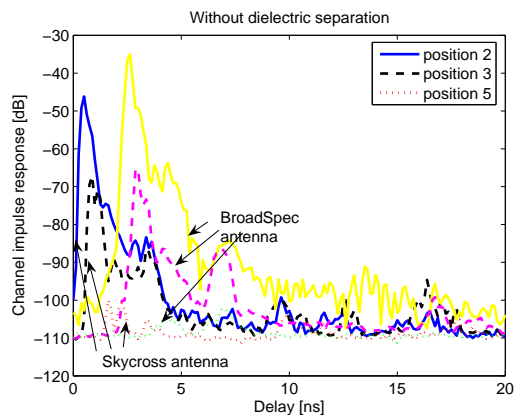


Fig. 6. Average channel impulse responses without dielectric separation. The Rx antenna is at the middle of the front torso and the Tx antenna is at level 1 positions 2, 3, and 5.

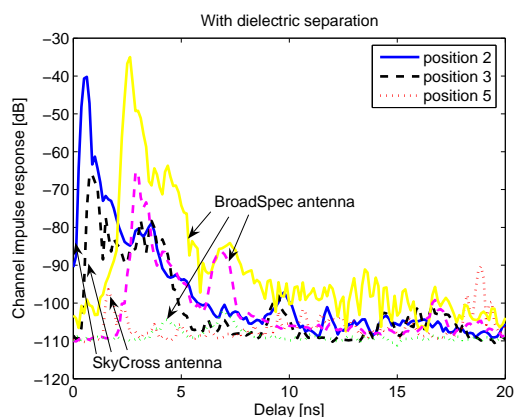


Fig. 7. Average channel impulse responses with dielectric separation. The Rx antenna is at the middle front of the torso and the Tx antenna is at level 1 positions 2, 3, and 5.

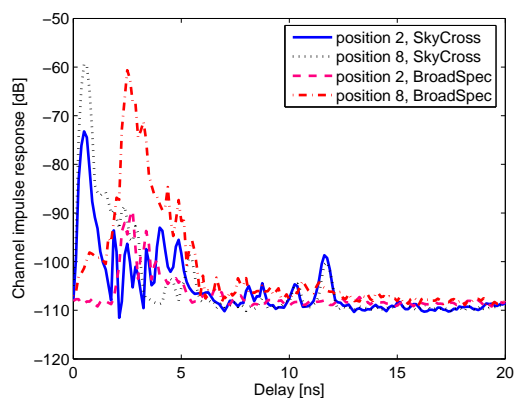


Fig. 8. Average channel impulse responses for the subject that has an artificial aortic valve implant. The Rx antenna is at the middle front of the torso and the Tx antenna is at level 1 position 2 and 8.

from the environment. The 1st set of measurements (around the body) were taken at two different levels of the torso, at the chest level (level 1) and at the abdomen level (level 2) as illustrated in Fig. 3. At each level, the Rx antenna (the rectangle in the figure) was fixed at the middle front of the torso and the Tx antenna (the circle in the figure) was placed at various positions at distances of 10 cm. The measurements for the subject who has a titanium alloy aortic valve implant [15-16] was also taken to see whether both types of antennas give the same type of results.

The 2nd set of measurements study the radio link between sensor nodes on the body shown as A1 in Fig. 1. The Rx antenna was at the middle front of the torso and the Tx antenna was placed on the left hand wrist. These locations are comfortable for most patients and they are possible places for antennas/transceivers connected to electrocardiogram (ECG) sensors and a pulse oximeter. With the equipment used in these experiments a single frequency domain measurement in the 3.1-10 GHz band takes several second. A real-time measurement of the radio channel fluctuations due to a body in motion is then not technically feasible. Instead, a pseudo-dynamic measurement method was applied, where each position in a walking cycle shown in Fig. 4 was kept still for the whole measurement period (e.g. 100 snapshots per position), and was modified according to the walking cycle.

Fig. 5 shows the positions of the 3rd set of measurements, where the Tx antenna was at the left-side of the waist. The subject was facing the Rx antenna placed on a 2-m high wall. This emulates the channel link A2 in Fig. 1. A pseudo-dynamic measurement covering a walking cycle was again applied for this set of measurements.

III. RESULTS ANALYSIS

One hundred individual realizations of the channel impulse responses were measured and averaged for each position. Since the energy of these responses close to the human body decays rapidly we focus only on the first 20 ns of each channel impulse response. Figs. 6 and 7 show the average channel impulse responses for the 1st set, level 1 comparing both types of antennas, when the antennas are directly attached to the clothes and when there is a dielectric separation between the body and the antenna, respectively. As it can be seen, the results from both antennas have the same trend. However, for the SkyCross antennas the first peaks of the channel impulse responses arrive earlier. The explanation is that the SkyCross antennas have a higher gain between them than the P200 BroadSpecTM antennas according to their antenna patterns [13, 14]. Moreover, the SkyCross antenna has a good matching property (VSWR mentioned before) through a larger frequency range than the one of the P200 BroadSpecTM antenna. The average channel impulse response of the subject with an aortic valve implant drops off more quickly for both types of antennas cases as illustrated in Fig 8. Figs. 9 (a) and (b) show the average of the magnitude of the channel impulse responses for each position in a walking cycle in the 2nd set comparing both types of antennas. It can be seen that the arm

TABLE I
RMS DELAY SPREAD τ_{RMS} AND AMPLITUDE DISTRIBUTION OF THE MEASUREMENTS COMPARING TWO TYPES OF ANTENNAS.

Measurement scenario	RMS delay spread		Amplitude distribution	
	Mean [ns]	Std [ns]	Delay bin 1	Delay bin 5
Set 1: position 2, SkyCross	0.0870	0.0559	log-normal	log-normal
position 2, BroadSpec TM	0.1863	0.0670	log-normal	log-normal
position 3, SkyCross	0.2071	0.0570	log-normal	log-normal
position 3, BroadSpec TM	0.4197	0.0670	log-normal	log-normal
Set 2: Rx at the middle front of the torso				
static: Tx at the left wrist, SkyCross	0.2087	0.0559	log-normal	log-normal
pseudo-dynamic: Tx at the left wrist, SkyCross	0.1371	0.0670	Weibull	Weibull
static: Tx at the left wrist, BroadSpec TM	1.5992	0.5485	log-normal	log-normal
pseudo-dynamic: Tx at the left wrist, BroadSpec TM	0.8782	0.7299	Weibull	Weibull
Set 3: Tx at the left waist				
static: facing Rx, SkyCross	0.0839	0.0086	log-normal	log-normal
pseudo-dynamic: facing Rx, SkyCross	0.0998	0.0301	Weibull	log-normal
static: facing Rx, BroadSpec TM	0.0896	0.0092	log-normal <td log-normal	
pseudo-dynamic: facing Rx, BroadSpec TM	0.1008	0.0233	Weibull	log-normal

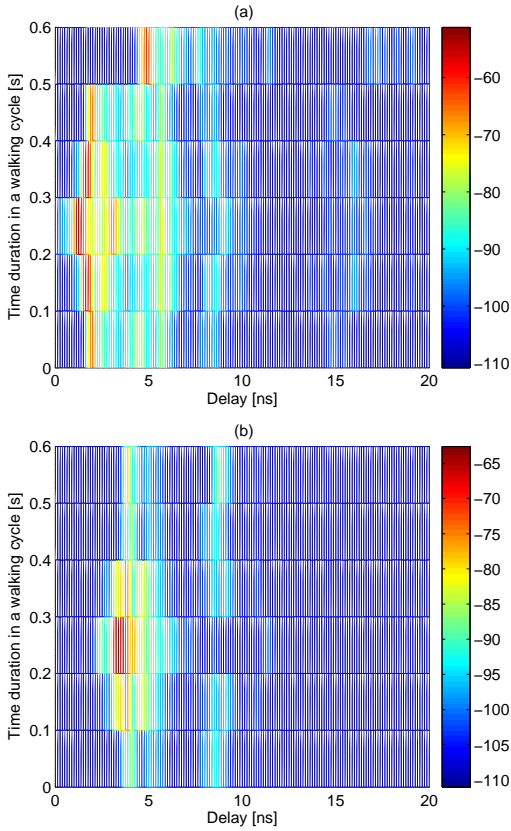


Fig. 9. Magnitude of the channel impulse responses for each position in a walking cycle in the 2nd set: (a) SkyCross SMT-3TO10M-A antennas and (b) P200 BroadSpecTM antennas.

movement during a walking cycle has a significant impact on the radio link between the Tx antenna on the left wrist and the Rx antenna at the middle front of the torso. For instance, when the left hand moves to the uppermost in the position three, the strongest path arrives earlier than in the other positions due to the shorter distance between both antennas. There are also more significant paths due to the reflection of the wave out of the arm and the shoulder. The shadowing due to blocking

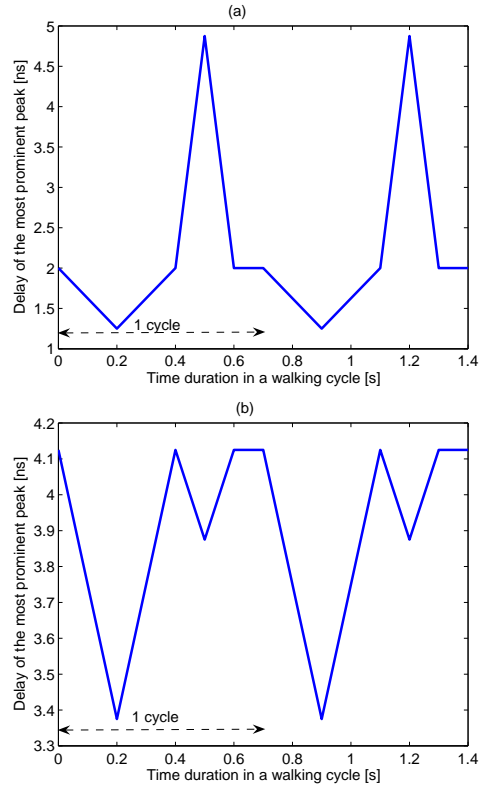


Fig. 10. Delay of the most prominent peak of the impulse responses for each position in a walking cycle in the 2nd set: (a) SkyCross SMT-3TO10M-A antennas and (b) P200 BroadSpecTM antennas.

of the body is shown in position six, where the left hand moves to the lowermost location. The results from both types of antennas are similar. Figs. 10 and 11 show the delay and the amplitude of the most prominent peak of the impulse responses during a walking cycle, respectively. Again, the shorter delays of the channel impulse responses can be observed when using the SkyCross antennas. The variability in amplitude and delay, if ignored, can cause degradation in the performance of the medium access control (MAC) layer. Moreover, this variability

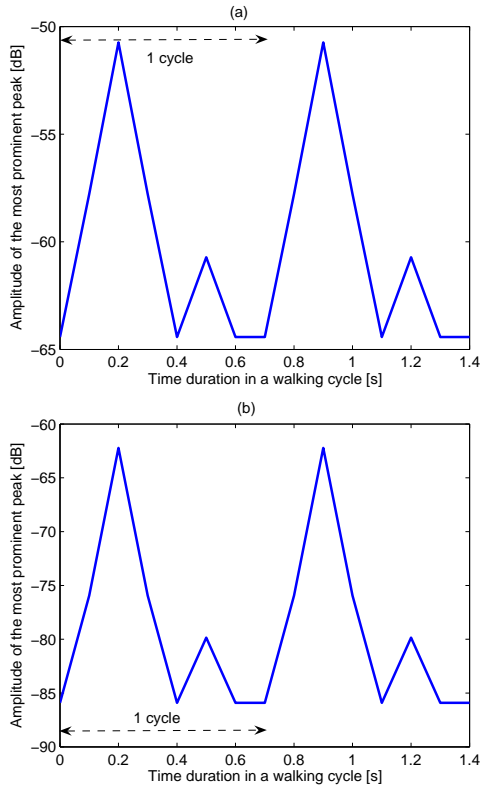


Fig. 11. Amplitude of the most prominent peak of the impulse responses for each position in a walking cycle in the 2nd set: (a) SkyCross SMT-3TO10M-A antennas and (b) P200 BroadSpecTM antennas.

depends heavily on the position of the sensor, the body and the antennas.

We evaluate the delay dispersion within the channel in terms of the root mean square (RMS) delay spread τ_{RMS} . To calculate it, all measured channel impulse responses are first truncated above the noise threshold set to four times of the noise standard deviation, i.e., -108.2 dB. The dynamic range varies depending on the different cases of the measurements. The means and standard deviations of the RMS delay spreads of each measurement set are summarized in Table I. The value of the RMS delay spreads depends on the probability of having shadowing due to blocking by the body and also the distance between the Tx and the Rx antennas. For example, in the 2nd set of the measurements, the static case has higher RMS delay spread than the pseudo-dynamic case, since the Tx antenna periodically gets closer to the Rx antenna. In addition, the standard deviations of the RMS delay spreads in the pseudo-dynamic cases are always larger than the ones in the static cases.

We summarize the distribution of the amplitudes of the first delay bin and the fifth delay bin in Table I. In the static cases, the amplitudes of channel impulse responses are log-normally distributed. On the other hand, the Weibull distribution is the most appropriate distribution for most cases in the pseudo-dynamic situations.

IV. CONCLUSIONS

We have conducted a series of UWB WBAN measurements in the frequency range of 3.1-10 GHz comparing two different types of antennas: the SkyCross SMT-3TO10M-A and the P200 BroadSpecTM antennas. The results for both types of antennas have a similar trend. Nonetheless, the SkyCross antennas are more attractive in WBAN applications because of their smaller size, the shorter delays of their impulse responses and a very good matching in a larger range in the UWB frequency band. The body motion effects were also investigated. If ignored, the fluctuations of the radio channels under such dynamic situations can cause severe performance problems in system design. A pseudo-dynamic measurement method was applied since a real-time measurement of the radio channel fluctuations due to the body movement is not technically feasible over a frequency band of several GHz. We can see the Weibull distribution is the most appropriate distribution for most cases in the pseudo-dynamic situations.

REFERENCES

- [1] P. Coronel, W. Schott, K. Schwieger, E. Zimmermann, T. Zasowski, H. Maass, I. Oppermann, M. Ran, and P. Chevillat, "Wireless body area and sensor networks," in *Proc. Wireless World Research Forum (WWRF) Briefings*, Dec. 2004.
- [2] State-of-the-Art Telemedicine/Telehealth: An International Perspective. Mary Ann Liebert, Inc., 2 Madison Avenue, Larchmont, NY 10538.
- [3] R. J. Cramer, R. A. Scholtz and M. Z. Win, "An Evaluation of the Ultra-Wideband Propagation Channel," *IEEE Trans. Antennas Propagation*, vol. 50, no. 5, pp. 561-570, May 2002.
- [4] S. Gezici and Z. Sahinoglu, "Theoretical Limits for Estimation of Vital Signal Parameters Using Impulse Radio UWB," *IEEE Communications Society subject matter experts for publication in the ICC 2007 proceedings*, 2007.
- [5] S. S. Ghassemzadeh and V. Tarokh, "The Ultra-Wideband Indoor Path Loss Model." Tech. Rep. P802.15 02/277r1SG3a, AT&T Labs, Florham Park, NJ, USA (IEEE P802.15 SG3a contribution, June 2002).
- [6] B. Kannan et al., "Characterization of UWB Channels: Large-Scale Parameters for Indoor and Outdoor Office Environment," IEEE P802.15 Working Group for Wireless Personal Area Networks (WPANs) (IEEE 802.15-04-0383-00-04a, July 2004).
- [7] M. Klemm and G. Troester, "EM Energy Absorption in the Human Body Tissues due to UWB Antennas," in *Electromagnetics Research*, PIER 62, 261-280, 2006.
- [8] A. Alomainy, Y. Hao, Y. Yuan, and Y. Liu, "Modelling and Characterisation of Radio Propagation from Wireless Implants at Different Frequencies," in *Proc. European Conference on Wireless Technology*, Sep. 2006.
- [9] T. Zasowski, F. Althaus, M. Stäger, A. Wittneben, and G. Tröster, "UWB for Noninvasive Wireless Body Area Networks: Channel Measurements and Results," in *Proc. IEEE Conference on Ultra Wideband Systems and Technologies (UWBST)*, Nov. 2003.
- [10] A. Fort, C. Desset, J. Ryckaert, P. De Doncker, L. Van Biesen, and P. Wambacq, "Characterization of the Ultra Wideband Body Area Propagation Channel," in *Proc. International Conference ICU*, pp. 22-27, 2006.
- [11] <http://www.alliancetesteq.com/>.
- [12] <http://skycross.com/Products/PDFs/SMT-3TO10M-A.pdf>.
- [13] TimeDomain Corporation, n.d., P210 Integratable Module Data Sheet, 320-0095 Rev B, TimeDomain Corporation, Huntsville, AL.
- [14] <http://www.hubersuhner.com>.
- [15] A. Taparugssanagorn, C. Pomalaza-Ráez, A. Isola, R. Tesi, M. Hämmäläinen, and J. Iinatti, "UWB Channel Study for Wireless Body Area Networks in Medical Applications," submitted to *IEEE Trans. Information Technology in BioMedicine*.
- [16] A. Taparugssanagorn, C. Pomalaza-Ráez, A. Isola, R. Tesi, M. Hämmäläinen, and J. Iinatti, "UWB Channel Modelling for Wireless Body Area Networks in Medical Applications," in *Proc. International Symposium on Medical Information and Communication Technology (ISMICT)*, Feb. 2009.